Titre: Title:	Extensional viscosity of coating colors and its relation with jet coating performance
Auteurs: Authors:	A. Arzate, G. Ascanio, Pierre J. Carreau et Philippe A. Tanguy
Date:	2004
Type:	Article de revue / Journal article
Référence: Citation:	Arzate, A., Ascanio, G., Carreau, P. J. & Tanguy, P. A. (2004). Extensional viscosity of coating colors and its relation with jet coating performance. *Applied Rheology*, *14*(5), p. 240-250. doi:10.1515/arh-2004-0013

Titre de la revue: Journal Title:	Applied Rheology (vol. 14, no 5)
Maison d'édition: Publisher:	Walter de Gruyter
URL officiel: Official URL:	https://doi.org/10.1515/arh-2004-0013
Mention légale: Legal notice:	

Extensional Viscosity of Coating Colors and its Relation With Jet Coating Performance

A. Arzate, G. Ascanio, P.J. Carreau and P.A. Tanguy*

Center for Applied Research on Polymers (CRASP), Department of Chemical Engineering, Ecole Polytechnique, P.O. Box 6079, Station Centre-ville, Montreal, Quebec H3C 3A7, Canada

*Email: philippe.tanguy@polymtl.ca
Fax: x1.514.340.4105

Received: 10.5.04, Final version: 9.8.04

Abstract:
An orifice flowmeter was used to measure the extensional viscosity of several non-pigmented fluids and paper coating colors containing calcium carbonate as pigment in the context of a jet coating application. The orifice flowmeter was first calibrated in terms of a dimensionless Euler number versus Reynolds number curve with Newtonian fluids. The calibration curve was then used to determine the apparent extensional viscosity of coating colors. In the strain rate range investigated, all the fluids were found to exhibit strain-thinning and the Trouton ratio of the coating colors was in the range 5 to 20. Jet coating tests were also carried out in order to evaluate the effect of the extensional viscosity on the jet performance. The extensional viscosity was shown to be a key parameter determining the configuration of the downstream meniscus in the web contact region.

Zusammenfassung:
Ein Düsenrheometer wurde benutzt um die Dehnviskosität von mehreren nicht pigmenthaltigen Flüssigkeiten und Papierfarbbeschichtungen mit Kalziumkarbonat als Pigment in Bezug auf die Jet-Beschichtungen zu untersuchen. Das Rheometer wurde zunächst mit newtonschen Flüssigkeiten mittels der Auftragung von Euler- gegen Reynoldsnummer kalibriert, so dass im Anschluss die scheinbare Dehnviskosität der Farbbeschichtungen bestimmt werden konnten. In dem untersuchten Dehnratenbereich zeigten alle Proben ein scherverdünnendes Verhalten mit einem Troutonverhältnis von 5 zu 20. Den Einfluss der Dehnviskosität auf die eigentlichen Jet-Beschichtung wurde in Folge untersucht, wobei gezeigt werden konnte, dass sie der Schlüsselparameter zur Kontrolle des Ablösemeniskuses von Substrat ist.

Résumé:
Un rhéomètre à orifice a été utilisé pour mesurer la viscosité extensionnelle de plusieurs fluides non pigmentés et de sauces de couchage prépareés à base de carbonate de calcium dans le cadre d'une application de couchage par jet. Le rhéomètre à orifice a été tout d'abord étalonné en utilisant une courbe du nombre d'Euler en fonction du nombre de Reynolds avec des fluides newtoniens. Cette courbe d'étalonnage a par la suite été utilisée pour déterminer la viscosité extensionnelle apparente des sauces de couchage. Dans l'intervalle des vitesses de déformation étudié, tous les fluides ont montré une rhéofluidifiance en extension, le rapport de Trouton des sauces de couchage étant compris entre 5 et 20. Des essais de couchage par jet ont été aussi menés dans le but d'évaluer l'effet de la viscosité extensionnelle des sauces de couchage sur la performance du jet. Il s'est avéré que la viscosité extensionnelle est un paramètre clé déterminant la configuration du ménisque en aval de la région de contact sur le substrat.

Key words: Extensional viscosity, orifice flowmeter, entry pressure method, coating color, jet coating

DOI: 10.1515/arh-2004-0013

INTRODUCTION

e paper coating process is a complex procedure at involves a paper web, a coating liquid and a etering device. The aim of coating is to improve e optical and printing properties of paper by plying a thin liquid film onto its surface. In ost coating operations, the control of both the ickness and the uniformity of the coated liquid m can be achieved using blade, roll and nozzle vices. Coating liquids also called colors are con-ntrated aqueous mixtures of dispersed miner- or synthetic particles (from 50 to 70 wt%), nders, dispersants, thickeners and other addi-ves [1]. Interactions between these various gredients are known to result in a complex rhe-ogical behavior [2].

The non-Newtonian behavior of coating lors depends also on flow kinematics during e application process and their deformation story. From a processing point of view, the owledge of their rheological behavior and the ntrol of this rheology are of practical interest, pecially the relationship between the rheolog-l properties and the ability of the fluid to coat a moving paper at high speed.

Jet coating is considered a promising chnology used as an alternative to traditional ooded nip, roll or blade coating. It can be per-rmed at speeds reaching 33 ms^{-1} [3, 4], yielding formation rates up to 10^4 s^{-1}. In this coating eration, the coating color is transferred to per by means of a nozzle (see Fig. 1). As soon as e liquid jet impinges onto the paper web, it is read on its surface as a pre-metered thin film. e thickness of the coated liquid film, T_f, is con-lled by the flow rate fed into the nozzle, which fines the jet thickness, T_j. The liquid flow in the plication region, and therefore the quality of e coated liquid film is strongly affected by oper-ing conditions, mainly the web speed, U, and e jet velocity, V, the liquid physical-chemistry d mechanical properties, and the nozzle rangement (D and α). The magnification of the plication region shown in Fig. 1 illustrates the evant characteristics of the jet field flow. There e regions of low deformation rate, in the feed-g nozzle and in the coated liquid film, and gions of extremely high deformation rate near e wetting contact line and over the down-eam meniscus. In the nozzle, a combination of ear and extensional flows is developed. In the

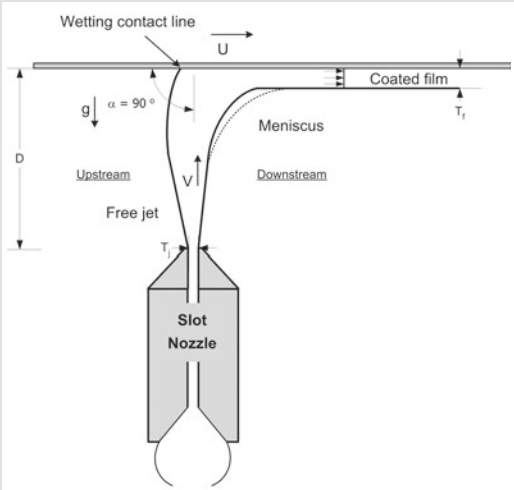

Figure 1: Magnification of application region.

coated liquid film, where plug flow is reached, the deformation vanishes. The flow close to the free surfaces is dominated by extension, then for a given paper speed, the downstream meniscus will exhibit different configurations according to the extensional properties of coating liquids. As shown in Fig. 1, i.e. a liquid having a low extensional viscosity will promote an increased curvature of downstream meniscus.

Because extensional flows strongly orient polymer molecules and non-symmetric particles, regions of extensional flow in jet coating process can have a strong effect on film application and final product properties [5], i.e. jet stability and stretching. Particles orientation could also have an effect on the printing properties [3]. Indeed, in extensional flow, the preferred molecular orientation is in the direction of the flow field because there are no competing forces to cause rotation as in shear flow. Hence, extensional flow will induce the maximum stretching of the molecules producing a chain tension that may result in a large resistance to deformation compared to shear flow.

Although the extensional viscosity is of fundamental importance for a variety of coating phenomena, the attention has rather been focused on the shear viscosity and viscoelastic properties of colors and suspensions. At present, no simple experimental technique exists to quickly and accurately measure the extensional viscosity of suspensions. Several innovative techniques have been developed for polymer melts and solutions [5]. However, the extensional properties have been difficult quantities to measure at high extensional rates.

The use of entry flows appears to be a good alternative when the fluid is submitted to strain rates larger than 1000 s^{-1}. The pioneering analysis of converging flow developed by Cogswell [6] is perhaps the most robust technique followed by the similar energy balance

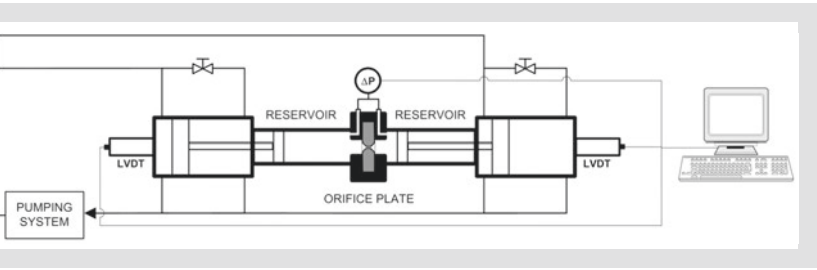

Figure 2 (left): Schematic diagram of the orifice flowmeter.

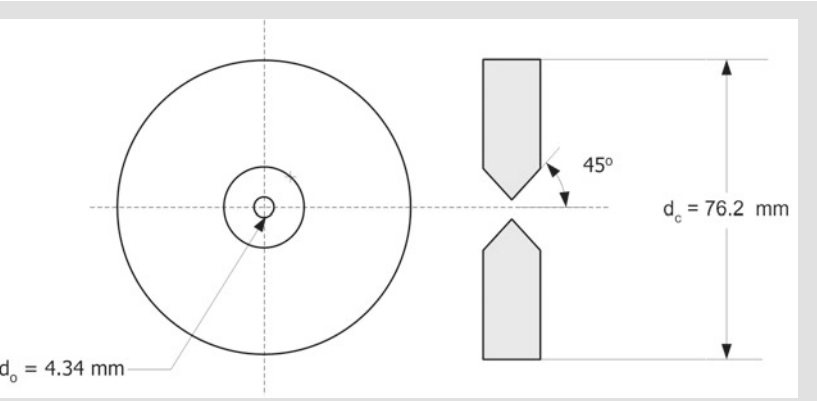

Figure 3 (right): Orifice plate.

minimization method of Binding [7]. The Cogswell method is based on the simple idea that the converging flow into an orifice has a strong extensional component and that extensional viscosity and extension rate can be calculated from entrance pressure drop using simple analytical expressions. It can be applied equally well to both high viscosity polymer melts and low viscosity polymer solutions.

Little information has been found on entry flow measurements for concentrated suspensions and coating colors. Isaksson et al. [8] evaluated the extensional properties for coating colors containing a blend of kaolin and calcium carbonate using a converging channel. Coating colors having an average solids content of 60wt % exhibited a strain-thinning at strain rates lower than 2000 s^{-1}. Della Valle et al. [9] used an orifice flowmeter for measuring the extensional viscosity of clay suspensions dispersed in aqueous polyethylene glycol having a solids content of 50, 55 and 60 wt%. They found that the extensional viscosity was constant for the three suspensions investigated, but 12 to 16 times larger than shear viscosity in a strain rate from 10 to 1000 s^{-1}. O'Brien and Mackay [10] measured the extensional viscosity of kaolin pigment suspensions (71 wt% solids content). They found that the strain-thickening became apparent at rates of 1000 s^{-1}. The ratio of the extensional to shear viscosity was found to have values of the order of 50 to 100. Ascanio et al. [11] found a Trouton ratio between 4 and 36 for coating colors based on clay at strain rates ranging from 1000 to 10000 s^{-1}. Depending on the coating color composition, extensional viscosity decreased or increased with increasing stain rate, and then leveled off at large strain rates.

The objective of this work is to investigate the extensional viscosity of typical paper coating colors at high strain rate, in conditions similar to those encountered in the jet coating process. Because extensional deformation dominates the jet flow in the application region, these data are used to elucidate the effect of extensional properties of the coating liquids on jet performance. The orifice flowmeter technique was used to measure the extensional viscosity of non-pigmented fluids and coating colors formulated containing calcium carbonate as in Ascanio et al. [11]. This method is based on the analysis of the extensional and simple shear components of the converging flow through a small size orifice and allows calculating the relationship between flow rate and pressure drop.

2 EXPERIMENTAL

2.1 MATERIALS

As shown in Fig. 2, the orifice flowmeter consists of two identical reservoirs separated by an orifice plate. The reservoirs are cylinders of 76.2 mm of inner diameter and 1 m long. The orifice plate is a disc with 45° converging and diverging sections which form a hole of 4.34 mm diameter (Fig. 3). Fluids are pushed through the orifice from one filled cylinder to the empty one in two-way direction by hydraulic pistons. The hydraulic system is driven by three different pumps. The speed of each piston is measured by means of a LVDT position transducer, allowing an accurate determination of the flow rate through the orifice (2.5 to 28 x 10^{-3} m^3 s^{-1}).

The operating principle of the orifice flowmeter is based on the pressure drop due to the flow through the orifice. The pressure drop is measured by means of a differential pressure transducer via small holes bored on each side of the orifice plate. A computer is used to control the pumps and collect flow data (the flow rate and the pressure drop through the orifice). For a full description of the background to the measuring technique, see Della Valle et al. [9] and Ascanio et al. [11].

2 OPERATING PRINCIPLE

converging flow of Newtonian fluid, in absence inertia effects, can be analyzed in terms of its tensional and simple shear components. The tal pressure drop, ΔP_T, for the converging sec-on can be defined only in terms of shear and tensional contributions as:

$$P_T = \Delta P_S + \Delta P_E \quad (1)$$

here ΔP_S is the pressure drop due to shear flow d ΔP_E is the pressure drop due to extensional w.

We assume that in the converging gion, the flow is laminar, locally fully-devel-ed and at steady state, the converging stream-es follow the actual cone angle of the orifice 5°) and the effect of the radial velocity is negli-ble. Furthermore it is considered that the pres-re drop is negligible in the divergent section of e orifice. Then for a Newtonian fluid, the pres-re drops induced by the shear flow and exten-onal flow are respectively:

$$P_S = \frac{2}{3}\mu\left(\frac{32Q}{\pi d_o^3}\right)\left(1-\left(\frac{d_o}{d_c}\right)^3\right) \quad (2)$$

$$P_E = \frac{16}{9}\mu\left(\frac{32Q}{\pi d_o^3}\right)\left(1-\left(\frac{d_o}{d_c}\right)^3\right) \quad (3)$$

here d_o and d_c are the diameter at the orifice d the cylinder, respectively, Q is the flow rate d μ is the shear viscosity of the fluid.

Considering that $d_o << d_c$, the total pres-re drop can be then written as:

$$P_T = \frac{22}{9}\mu\left(\frac{32Q}{\pi d_o^3}\right) \quad (4)$$

om Eqs. 2, 3 and 4 one can observe that shear d extensional contributions represent 27% and %, respectively, of the total pressure drop. This sult is valid for the orifice plate configuration used in this work, i.e. for an entrance angle equal to 45 degrees. The effective strain rate is taken as half the square root of the second invariant of the rate-of-deformation tensor, $\bar{\dot{\gamma}} = \sqrt{3}\,\dot{\epsilon}$ and was calculated by Della Valle et al. [9] in terms of the orifice diameter and the velocity at the orifice as:

$$\bar{\dot{\gamma}} = 29.1\left(\frac{V_o}{d_o}\right) \quad (5)$$

where V_o is the average velocity of the fluid at the orifice and the value of 29.1 is a geometrical constant obtained using Metzner and Otto concept [12] to relate the extensional rate to the shear rate.

2.3 CALIBRATION

The equipment was calibrated by plotting the pressure drop-flow rate curve in terms of dimensionless Euler number versus Reynolds number. The Reynolds number, *Re*, is here defined as:

$$\mathrm{Re} = \frac{d_o V_o \rho}{\mu} \quad (6)$$

and the Euler number, *Eu*, as:

$$Eu = \frac{\Delta P_T}{0.5\rho V_o^2} \quad (7)$$

By combining Eqs. 4, 6 and 7, the orifice curve can be described in laminar regime by the relation:

$$Eu = \frac{39.11}{Re} \quad (8)$$

Eq. 8 represents the theoretical expression of *Eu* versus *Re* for the laminar regime. This expression has been verified for Newtonian fluids [9, 10] and by a 2-D flow simulation [9].

The calibration curve can be used to determine the apparent extensional viscosity of non-Newtonian fluids from the knowledge of the pressure drop. In the case of a purely shear-thinning (or shear-thickening) fluid, the shear viscosity in the definition of Reynolds number (Eq. 6) is considered as an apparent viscosity evaluated at the shear rate occurring at the orifice. Then, relating the shear viscosity to the extensional viscosity by the Trouton ratio (i.e. $\eta_E = 3\mu$), the apparent extensional viscosity can be obtained from the pressure drop using the orifice curve in the laminar regime (Eq. 8) as:

$$\eta_E = \frac{6}{39.11}\Delta P_T \left(\frac{d_o}{V_o}\right) \tag{9}$$

It is important to point out that as the strain rate increases, the inertia effects in the orifice flow can no longer be neglected and the data need to be corrected. According to Ascanio, et al. [11], pressure forces are equal to inertia forces for Reynolds numbers larger than 20, so that Euler number becomes equal to unity. Hence, the Euler number used to calculate the apparent extensional viscosity in this region is corrected as follows:

$$Eu_{corr} = Eu - 1 \tag{10}$$

Three concentrations of polyethylene glycol (PEG 35 000, Clariant Ltd.) aqueous solutions ranging from 20 to 30 wt% were used as Newtonian fluids for calibrating the orifice flowmeter. The corresponding viscosities were 0.14, 0.35 and 0.59 Pa s for 20, 25 and 30 wt% solutions, respectively.

Table 1: Dried composition of coating colors (pph of pigment basis).

Ingredients	Coating color					
	C55-05	C55-1	C65-0	C65-05	C55-05L	C65-0L
Carbital 90 [pph]	100	100	100	100	100	100
Latex CP620NA [pph]	-	-	-	-	10	10
CMC Finnfix 10 [pph]	1	1	1	1	1	1
CMC 7LT [pph]	0.5	1	-	0.5	0.5	-
Solids content [wt %]	55	55	65	65	55	65
Density [kg m^{-3}]	1528	1525	1690	1702	1462	1466

2.4 FLUIDS

Two types of fluids were compared in this work: non-pigmented fluids and pigmented coating colors. A carboxymethyl cellulose (Finnfix 30, Noviant Inc.) aqueous solution at 6 wt% having a density of 1020 kg m^{-3} and an aqueous solution of 5 wt% polyethylene glycol (PEG 35000, Clariant Ltd) - 3 wt% carboxymethyl cellulose (Finnfix 700, Noviant Inc.) having a density of 1009 kg m^{-3} were used as non-pigmented non-Newtonian fluids. In the forthcoming results, the fluids will be denoted by PEG, FF30 or FF700 followed by one or two digits indicating the concentration by weight.

Six coating colors based on commercial paper formulations were tested in the orifice flowmeter. Ground calcium carbonate (Carbital 90) from Imerys was used as pigment. A carboxymethyl cellulose with an average molecular mass of 60000 (Finnfix 10) from Noviant Inc. was used as thickener and water retention aid. Modified styrene butadiene latex (CP620NA) from Dow Chemical Co. was used as a binder, and sodium carboxymethyl cellulose having an average molecular mass of 90000 (CMC 7LT) from Hercules was used as a thickener agent. Each coating color was prepared from the pigment slurries adding gradually 1 pph (dry parts of ingredient per hundred parts of pigment) of Finnfix10, previously hydrated and, then, 10 pph of latex was added to the same formulation. According to the formulations shown in Tab. 1, two different contents (0.5 or 1 pph) of CMC 7LT were also added at the same time as Finnfix10. The final pH was adjusted between 8.5 and 9.0 by adding 10 wt% NaOH and the final solids content was adjusted to 55 or 65 wt%. In the presentation of the results, all the colors ("C") will be denoted by a code containing three symbols. The first symbol, 55 or 65, represents the solids content. The second symbol, 0, 0.5 or 1, denotes the added amount of CMC and the third symbol, L, indicates the latex addition, as indicated in Tab. 1. All the fluids were tested the day following their preparation.

Steady and oscillating shear rheological tests were performed with a rotational rheometer (Advanced Rheometer AR-2000, TA Instruments). The steady shear viscosity, storage modulus, G' and loss modulus, G'' were all measured in a Couette configuration of 30 mm for outer cylinder and 28 mm for the inner cylinder for all fluids. The measurements were performed at 25 °C.

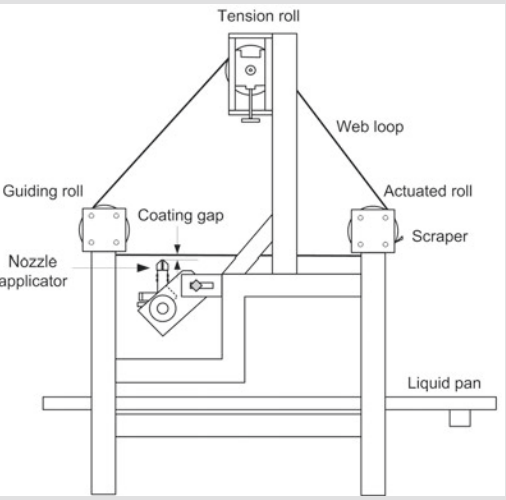

Figure 4 (left): Sketch of the laboratory jet coater.

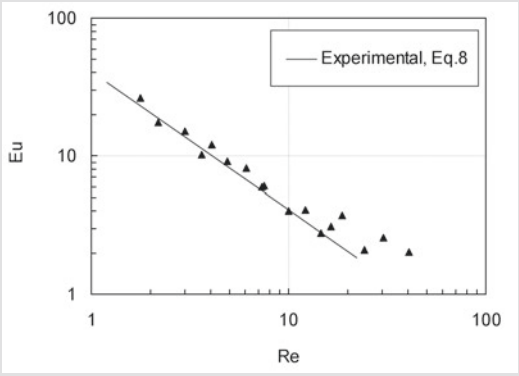

Figure 5 (right above): Calibration curve in terms of the dimensionless Euler number versus Reynolds number for Newtonian fluids.

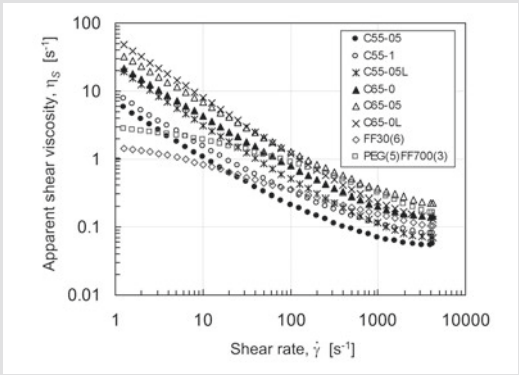

Figure 6 (right below): Steady shear viscosity as a function of shear rate for all the fluids.

JET COATING TESTS

ating studies were carried out on the laborato- jet coater shown in Fig. 4. The coater is com- sed of a slot-type nozzle applicator and a mov- g synthetic paper loop (1058-Tyvek™). The nozzle plicator transfers the coating liquid to the web, thout overflow or post-metering. The nozzle s a slot of 2 mm thick and a width of 100 mm. all the experiments, the distance between the zzle exit and the web also called coating gap, *D*, as kept at 5 mm and the impingement angle, α, 90 degrees (see Fig. 4). The web speed, *U*, can varied from 0 to 25 m s^{-1}.

For the purpose of this study, a good jet rformance for a given web speed was defined the minimum flow rate which allows devel- ing a stable jet. The jet was visualized in the ating gap under steady-state flow conditions ing a color video camera (Hitachi VK-C370) and ideo recorder (Hitachi D4A MX431).

RESULTS AND DISCUSSION

CALIBRATION

g. 5 shows the calibration curve (Euler number rsus Reynolds number) experimentally estab- hed. In the range of pressure drop values mea- red, the accuracy was estimated to be ± 3.2 % d ± 12.8 % for the *Re* and *Eu*, respectively. A lam- ar region (slope of -1) is observed at low *Re*, here the flow is purely viscous. At high *Re*, iner- effects become important and the pressure op becomes gradually independent of the vis- sity. The critical *Re* corresponding to the tran- ion flow regime was established at 20. Hence, ta obtained for *Re* > 20 were corrected using . 10. In laminar region, the experimental cali- ation curve can be correlated by:

$$Eu = \frac{40.7}{Re} \qquad (11)$$

This is not significantly different from the theoretical expression (Eq. 8).

3.2 SHEAR FLOW RESULTS

Non-pigmented fluids and coating colors exhibited a shear-thinning behavior, which can be well described by a power-law model with an infinite shear viscosity at high shear rate, namely:

$$\eta_s = m\dot{\gamma}^{n-1} + \eta_\infty \qquad (12)$$

Table 2: Power-law parameters of all the fluids.

Fluid	Consistency index (*m*) [Pa s^n]	Shear power-law index (*n*)	η_∞ [Pa s]
FF30(6)	1.69	0.66	0.104
PEG(5)FF700(3)	3.63	0.68	0.160
C55-05	5.22	0.34	0.056
C55-1	7.07	0.37	0.100
C55-05L	19.46	0.23	0.070
C65-0	22.26	0.30	0.143
C65-05	33.78	0.32	0.225
C65-0L	52.43	0.20	0.130

where η_s is the apparent shear viscosity, $\dot{\gamma}$ is the shear rate, η_∞ is the infinite shear viscosity and *m* and *n* are the shear consistency and the shear power-law index, respectively.

Fig. 6 shows the typical shear viscosity curves for all the coating colors in the shear rate range of 1 to 4300 s^{-1}. All the fluids exhibited a shear-thinning behavior in the shear rate range of interest, that is $\dot{\gamma} > 30\ s^{-1}$. The rheological parameters *m*, *n* and η_∞ are reported in Tab. 2. The rheological parameters of non-pigmented fluids estimated in the shear rate region of interest are presented as references in the same table. From Fig. 6, it is observed that a constant shear viscosity for all the coating colors could be reached for shear rate higher than 3000 s^{-1}. The effect of latex addition is more evident at low shear rate (see the data sets for C55-05L/C55-05 and C65-0L/C65-0). At high shear rate, the addition of latex does not significantly affect the shear viscosity. However, the shear rate to which viscosity is not sensitive to the addition of latex depends on the solids content. Typically the addition of latex decreases the shear viscosity at high shear rates. Indeed, smaller latex particles (average particle size of 0.1 μm) could fit between the larger pigments particles (average particle size of 2 μm) and lubricate the flow of the larger particles [13].

Several additional remarks can be made from Tab. 2 and Fig. 6. The shear power-law index remains within a relatively narrow range but increases slightly with the thickener concentration and reduces with latex addition. The shear consistency index is shown to increase with thickener concentration, solids content and latex addition. However, the effect of latex on the infinite shear viscosity is more complex: for the high solids content coatings, the addition of latex results in a reduction of the infinite shear viscosity as discussed above. No shear-thickening behavior at high shear rate was observed with any formulation in the shear rate range investigated.

It has been demonstrated that the elastic effects of high concentrated coating colors can be neglected when the fluid is highly deformed [14]. The results of our oscillatory shear measurements are summarized in Tab. 3, where the loss modulus, *G''* and the storage modulus, *G'* evaluated at a strain rate amplitude of 10 are reported. It can be seen that the loss factor, $\tan\delta = G''/G'$, is considerably larger than 1, indicating that all the fluids investigated were much more viscous than elastic. The critical strain amplitude, γ_c, at which moduli depart from a linear behavior is the same for all the coating colors and refers to the strain to which the coating colors can withstand without being perturbed. In Tab. 3, it can be seen that the coating colors have a critical strain amplitude of 0.004 that is considerably lower than that for non-pigmented fluids (0.25). It means that internal structure of the coating colors begins to break down more easily than that of non-pigmented fluids. The elastic behavior of the coating colors is probably the result of a weak network structure between pigment particles and/or thickener. At low strain amplitude, below the critical point, both moduli are constant. From this critical point the moduli decrease when increasing strain amplitude and the fluids start exhibiting a non-linear viscoelastic behavior.

Table 3: Dynamic data at 1 Hz and apparent extensional viscosity data evaluated at $\overline{\dot{\gamma}} = 4200\ s^{-1}$.

Fluid	Critical strain (γ_c)	Loss modulus (G'')[1] [Pa]	Storage modulus (G')[1] [Pa]	η_E [Pa s]
FF30(6)	0.25	2.54	0.38	2.10
PEG(5)FF700(3)	0.25	7.07	0.72	2.31
C55-05	0.004	2.03	0.02	0.46
C55-1	0.004	2.81	0.01	0.99
C55-05L	0.004	5.39	0.05	0.78
C65-0	0.004	11.75	2.50	2.54
C65-05	0.004	14.84	2.81	2.91
C65-0L	0.004	29.29	6.95	2.50

[1] Moduli were evaluated at strain amplitude of 10.

3.3 EXTENSIONAL FLOW RESULTS

In Figs. 7 and 8, the apparent extensional viscosity data are plotted as a function of the effective strain rate. The apparent extensional viscosity and effective strain rate were calculated using Eq. 9 and 5, respectively. All data for *Re* > 20 were corrected using Eq. 10. An average accuracy of 15% was estimated for the apparent extensional

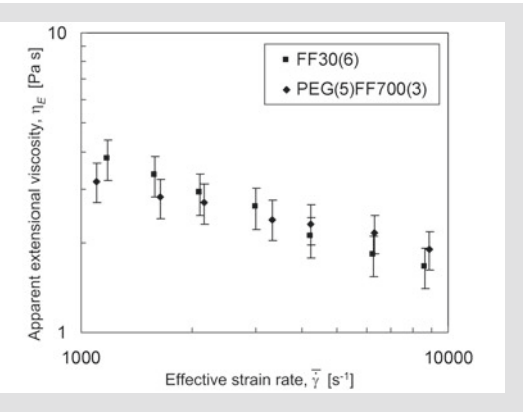

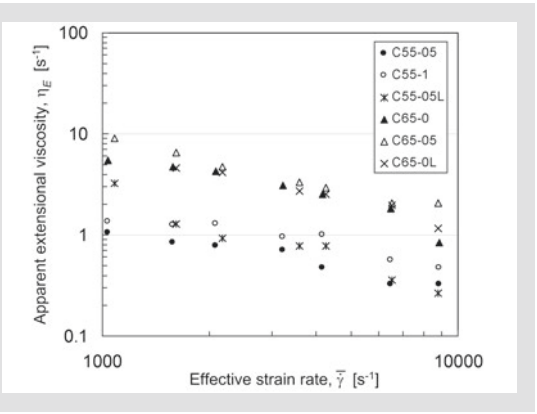

Figure 7 (left): Apparent extensional viscosity as a function of effective strain rate for non-pigmented fluids.

Figure 8 (right): Apparent extensional viscosity as a function of effective strain rate for all the coating colors.

scosity measurements. Fig. 7 shows the appar-t extensional viscosity obtained for the non-gmented fluids FF30(6) and PEG(5)FF700(3). th fluids are strain-thinning in the effective ain rate investigated, i.e. the apparent exten-nal viscosity decreases with increasing effec-e strain rate.

As Fig. 8 shows, the three low solids con-nt coating colors exhibited a similar behavior. initial plateau at low effective strain rate ove 2000 s^{-1}) is observed. Then, coating colors hibit strain-thinning with increasing effective ain rate. At a given strain rate, an increase in the ckener content (CMC 7LT) leads to an increase the apparent extensional viscosity. A certain nsitivity to the latex addition is also observed. gh solids content colors also exhibit strain-thin-ng in the whole range of the effective strain rate vestigated (Fig. 8). In this case, the apparent tensional viscosity is not sensitive to latex addi-n (see C65-0 and C65-0L). The amount of thick-er slightly affects the extensional viscosity at w effective strain rate (see C65-0 and C65-05).

r all the fluids, the apparent extensional viscos-, η_E, can be described with a power-law function the effective strain rate, $\dot{\bar{\gamma}}$, as follows:

$$= e\dot{\bar{\gamma}}^{t-1} \qquad (13)$$

here e and t are the extensional consistency d extensional power-law index, respectively.

In order to compare the extensional operties of the fluids investigated, the appar-t extensional viscosity data evaluated at $\dot{\bar{\gamma}}$ = 00 s^{-1} are shown in Tab. 3. This effective strain e value corresponds to the average value of e extension rate occurring in the application gion of the jet coater where the extension rate defined as the ratio of the difference of the web eed and the jet velocity to the difference of the m thickness and the jet thickness:

$$= \frac{U-V}{T_f-T_j} \qquad (14)$$

The same order of magnitude of η_E (around 2.5 Pas) is observed for non-pigmented fluids and high concentrated coating colors. It means that, from a mechanical point of view, both kinds of fluids would have the same ability to develop jets during jet coating process. The molecular nature of the thickener used may significantly influence the extensional flow behavior. Branched molecules of non-pigmented fluids (carboxymethyl cellulose) would be at the origin of a high extensional viscosity, since they exhibit a randon-coil type conformation in solution [15]. In the case of highly concentrated coating colors, it is possible that the alignment of the particles influences the apparent extensional viscosity value. With comparable operating conditions, low concentrated coating colors would promote the stretching of the jet, generating thus thinner jets, as these fluids would offer less resistance to the stretching.

On the other hand, the apparent extensional viscosity increases with solids content. We can see in Tab. 3 that η_E of C65-05 is about six times larger than that of C55-05. For the low concentrated coating colors, the effect of thickener is more evident. For instance, C55-1 exhibits a η_E twice larger than that of C55-05 while C65-05 exhibits η_E only 15% larger than that exhibited by C65-0. Finally, it is observed that the addition of latex strongly affects η_E of low concentrated coating colors (i.e. it increases η_E). For high solids colors, the addition of latex changes the type of interactions and reduces η_E (compare C65-05 with C65-0L). It would seem that the effect of thickener is suddenly minimized by the latex addition.

3.4 TROUTOUN RATIO

It is interesting to compare the apparent extensional viscosity with the shear viscosity in terms of the Trouton ratio, which was calculated by the following expression:

$$Tr = \frac{\eta_E}{\eta_s} \qquad (15)$$

ure 9 (left): Trouton ratio a function of the effective rain rate for all the fluids.

Figure 10: Jet flow image from application region at $U = 12.5\ ms^{-1}$ with a) (right above) FF30 and b) (right middle) C55-1.

Figure 11 (right below): Downstream meniscus configuration for $U = 8.3\ ms^{-1}$.

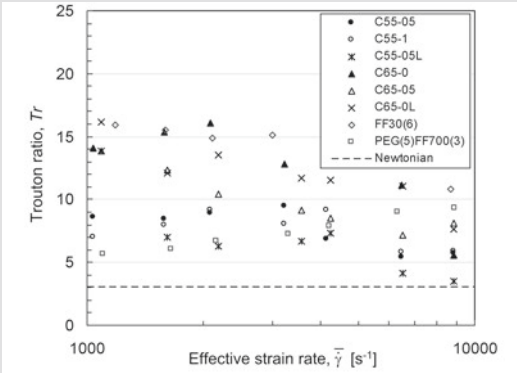

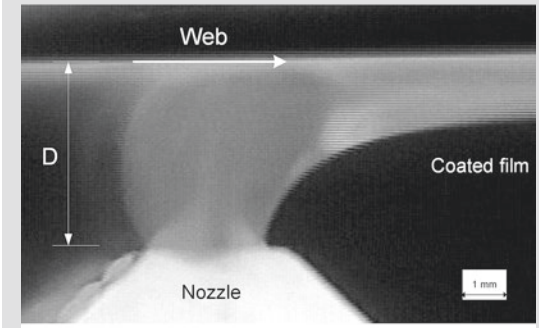

(a) FF30(6)

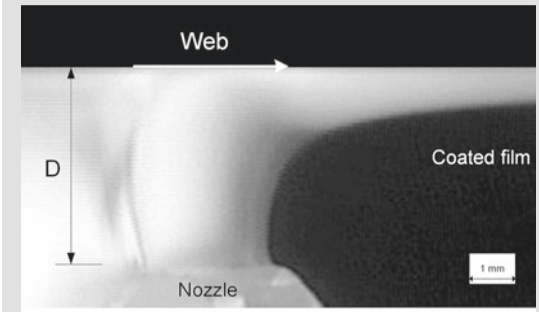

(b) CC55-1

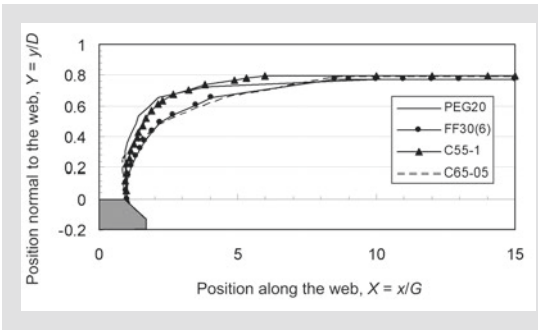

where η_E is the extensional viscosity data plotted in Fig. 8 and η_S is the apparent shear viscosity at the same value of the effective strain rate. It is important to point out that the shear viscosity was considered as a constant for $\dot{\gamma} > 3000\ s^{-1}$ reported in Tab. 2. The results for all the coating colors are presented in Fig. 9. The Trouton ratio is larger than the theoretical value of 3 for Newtonian fluids. For effective strain rates smaller than 3000 s^{-1} the high solids content colors show a *Tr* of about 15, while for the low solids colors *Tr* is about 10. In the effective strain range from 3000 to 6000 s^{-1}, this ratio is fairly constant and of the order of 10 for all the coating colors. *Tr* decreases down to 5 for effective strain rate larger than 6000 s^{-1}.

These values of the Trouton ratio are comparable to those obtained by Della Valle et al. [9] and Ascanio et al. [16] for clay suspensions in a Newtonian fluid containing 50 - 65 wt% solids content. Furthermore, these results are similar to the value obtained with coating colors based on delaminated kaolin clay (52 and 62 wt%) and ground calcium carbonate (55 and 65 wt%) by Arzate et al. [17] who found a Trouton ratio between 8 and 20. However, it has been found that the Trouton ratio could reach values of 85 for coating colors based on delaminated kaolin clay [16].

3.5 JET PERFORMANCE

Figs. 10a,b are examples of jet flows obtained in the application region with the non-pigmented fluid, FF30(6) and the low concentrated coating color, C55-1, respectively. These images correspond to stable jets obtained at $U = 12.5$ m s^{-1}. In comparable operating conditions, as it can be seen in Fig. 10, a liquid having a high extensional viscosity (FF30(6)) exhibited a less curved downstream meniscus (longer radius of curvature) than the low extensional viscosity liquid (C55-1). Consequently, the length necessary for the coated film to reach its final thickness is larger.

In order to compare the jet performance for four fluids in the same operating conditions, the downstream meniscus configuration obtained at $U = 8.3$ m s^{-1} is presented in Fig. 11. In this figure, *X* and *Y* represent dimensionless positions along the web and normal to the web, respectively. Half-gap of the nozzle slot, *G* and the width of the coating gap, *D* were used to represent the x-coordinate and y-coordinate scale, respectively. As expected, the curvature of the meniscus depends on the extensional viscosity. The curvature decreases with increasing extensional viscosity. This behavior is general to all the non-Newtonian fluids investigated. From a processing point of view, a low extensional viscosity seems to be beneficial for a good runnability since the coating liquid would exhibit less resistance to deformation, so the radius of curvature of the downstream meniscus would be reduced, as well as the liquid tearing. These results confirm that the extensional viscosity is relevant in evaluating the behavior of coating colors. In addition the effect of strain-thinning behavior was clearly observed at high web speed. Under these operating condi-

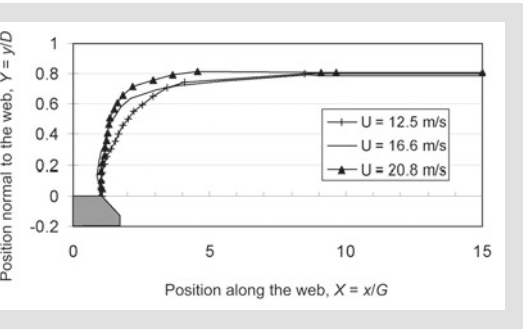

Figure 12: Downstream meniscus configuration for C65-o at three different web speeds.

ns, the downstream meniscus tends to recede th increasing web speed as illustrated in Fig. 12 r C65-o at three different web speeds (U = 12.5, 6 and 20.8 m s^{-1}). However, the observations of g. 12 could be largely due to inertia effects under ch high jet velocities.

ONCLUSION

this work, the apparent extensional viscosity non-pigmented fluids and coating color for-ulations containing calcium carbonate as pig-ent was determined at high strain rates typical jet coating process. For this purpose, an orifice owmeter, whose operating principle is based on e pressure drop-flow rate relationship for the w through a small size orifice, was used.

A strain-thinning behavior was served for all the coating liquids. The Trouton tio of the coating colors was found to be around for $\overline{\dot{\gamma}} < 6000$ s^{-1}. This result is in good agree-ent with to that reported in the literature for e high concentrated suspensions. In jet coat-g, the coating colors are submitted to exten-onal strain rates around 5000 s^{-1}, in the appli-tion region, so that the extensional viscosity uld reach values 10 times larger than shear vis-sity. This could be very useful information to plain some phenomena in jet coating process, ch as the jet stretching, the increase of the back w on the nozzle, the jet tearing preventing the tire coating film to be transferred to the web rface, etc. The extensional viscosity was found be slightly sensitive to the amount of thicken-but practically insensitive to the addition of tex. The amount of solids contained into the ating colors strongly affects the extensional scosity.

In addition, the extensional properties ere related to the jet stretching in the applica-on region via the downstream meniscus con-guration. Low extensional viscosity promotes increased curvature of the downstream eniscus. From a processing point of view, a low tensional viscosity is beneficial for a good nnability, since it increases the curvature of the ownstream meniscus and consequently duces the distance required for the coated film to reach its final thickness. Finally, the results presented here should be regarded as estimates of the rheological properties in extension with the intention to better interpret the jet coating process hydrodynamics.

ACKNOWLEDGEMENTS

The financial support received from Natural Sciences and Engineering Research Council of Canada and Pulp and Paper Research Institute of Canada is gratefully acknowledged.

NOTATION

d_o	Diameter of the orifice [m]
d_c	Inner diameter of the cylinder [m]
D	Distance between the nozzle exit and the web [m]
Eu	Euler number
Eu_{corr}	Corrected Euler number
G	Half-gap of the nozzle slot [m]
G'	Storage modulus [Pa]
G''	Loss modulus [Pa]
e	Extensional consistency index [Pas^t]
m	Shear consistency index [Pasn]
n	Shear power-law index
Q	Flow rate through orifice [m^{3}s^{-1}]
Re	Reynolds number
t	Extensional power-law index
T_f	Thickness of the coated liquid film [m]
T_j	Jet thickness [m]
Tr	Trouton ratio
U	Web speed [ms^{-1}]
V	Jet velocity [ms^{-1}]
V_o	Average velocity of the fluid at the orifice [ms^{-1}]
x	Position along the web [m]
X	Dimensionless position along the web
y	Position normal to the web [m]
Y	Dimensionless position normal to the web
α	Impingement angle [°]
$\dot{\gamma}$	Shear rate [s^{-1}]
$\overline{\dot{\gamma}}$	Effective strain rate [s^{-1}]
γ_c	Critical strain amplitude
δ	Loss factor [-]
ΔP_E	Pressure drop due to the extensional flow [Pa]

ΔP_S	Pressure drop due to the shear flow [Pa]
ΔP_T	Total pressure drop for the orifice [Pa]
$\dot{\epsilon}$	Extension rate [s^{-1}]
η_E	Apparent extensional viscosity [Pas]
η_S	Apparent shear viscosity [Pas]
η_∞	Infinite shear viscosity [Pas]
μ	Newtonian shear viscosity [Pas]
ρ	Density of the fluid [kgm^3]

REFERENCES

[1] Walter JC: The Coating Process, TAPPI Press, Atlanta (1993).

[2] Russel NB, Saville DA, Schowalter WR: Colloidal Dispersions, Cambridge University Press, Cambridge (1989).

[3] Hiorns AG, Coggon L, Windebank M: Evaluation of the Jet Fountain Applicator in Blade Coating Systems for LWC Rotogravure, Coating Conference, TAPPI Proceedings (1999) 111-116.

[4] Roberts J, Lerche LH, Bauer W: How's Life with Free Jet?, Pulp Paper Europe 4(1999) 25-26.

[5] Macosko CW: Rheology: Principles, Measurements, and Applications, VCH Publishers, New York (1994).

[6] Cogswell FN: Converging Flow of Polymer Melts in Extrusion Dies, Polym. Eng. Sci. 12 (1972) 64-73.

[7] Binding DM: An Approximate Analysis for Contraction and Converging Flows, J. of Non- Newton. Fluid Mech. 27(1988) 173-189.

[8] Isaksson P, Rigdahl M, Flink P, Forsberg S: Aspects of the Elongational Flow Behaviour of Coating Colours, J. Pulp Pap. Sci. 24 (1998) 204-205.

[9] Della Valle D, Tanguy PA, Carreau PJ: Characterization of the Extensional Properties of Complex Fluids Using an Orifice Flowmeter, J. Non-Newton. Fluid Mech. 94 (2000) 1-13.

[10] O'Brien VT, MacKay ME: Shear and Elongational Flow Properties of Kaolin Suspensions, J. Rheol. 46 (2002) 557-571.

[11] Ascanio G, Carreau PJ, Brito-De La Fuente E, Tanguy PA: Orifice Flowmeter for Measuring Extensional Rheological Properties, Can. J. Chem. Eng. 80 (2002) 1189-1196.

[12] Metzner AB, Otto RE: Agitation of Non-Newtonian Fluids, AIChE J. 3(1957) 3-10.

[13] Toivakka M, Eklund D: Prediction of Suspension Rheology Through Particle Motion Simulation, Advanced Coating Fundamental Symposium, TAPPI Proceedings (1995) 161-177.

[14] Carreau PJ, Lavoie PA: Rheology of Coating Colors: A Rheologist Point of View, Advanced Coating Fundamental Symposium, TAPPI Proceedings (1993) 1-12.

[15] Steffe JF: Rheological Methods in Food Process Engineering, Freeman Press, Michigan, (1996).

[16] Ascanio G, Carreau PJ, Réglat O, Tanguy PA: Extensional Properties of Coating Colors at High Strain Rates in Relation with Misting, Advanced Coating Fundamentals Symposium, TAPPI Proceedings (2003) 5-8.

[17] Arzate A, Ascanio G, Carreau PJ, Tanguy PA: Extensional Properties of Coating Colors at High Strain Rates, ASME International Mechanical Engineering Congress and Exposition (2003) paper IMECE03-43529.